J Solid State Electrochem (2013) 17:2055–2060
DOI 10.1007/s10008-013-2069-4

ORIGINAL PAPER

A facile bubble-assisted synthesis of porous Zn ferrite hollow microsphere and their excellent performance as an anode in lithium ion battery

Lingmin Yao · Xianhua Hou · Shejun Hu · Qiang Ru · Xiaoqin Tang · Lingzhi Zhao · Dawei Sun

Received: 29 November 2012 / Revised: 14 March 2013 / Accepted: 17 March 2013 / Published online: 27 March 2013

Abstract Pure porous hollow Zn ferrite ($ZnFe_2O_4$) microspheres have been successfully synthesized by a facile bubble assisted method in the presence of ammonium acetate (NH_4Ac) as an anode material in lithium ion battery. The shape, size, and morphology of Zn ferrite are investigated by X-ray diffraction, scanning electron microscopy, and transmission electron microscopy. Furthermore, the probable bubble-assisted formation mechanism of porous hollow Zn ferrite spheres based on the experimental results is proposed. With the porous hollow structure, the obtained pure Zn ferrite particle as an anode in lithium ion battery demonstrates high capacity and excellent cycle ability. The high initial discharge specific capacity is approximately 1,400 mAh g^{-1} and a reversible specific capacity approaches 584 mAh g^{-1} after 100 cycles at a constant current density of 100 mA g^{-1}. The excellent electrochemical performance of the as-prepared Zn ferrite could be attributed to the special structure with which the volume expansion and pulverization of the particles became increasingly reduced.

Keywords Porous hollow sphere · Lithium ion battery · Anode materials · Zn ferrite

L. Yao · X. Hou · S. Hu · Q. Ru · X. Tang · D. Sun
School of Physics and Telecommunication Engineering, South China Normal University, Guangzhou 510006, People's Republic of China

L. Yao · X. Hou (✉) · S. Hu · Q. Ru · X. Tang · D. Sun
Engineering Research Center of Materials and Technology for Electrochemical Energy Storage (Ministry of Education), Guangzhou 510006, People's Republic of China
e-mail: houxh@scnu.edu.cn

L. Zhao
Institute of Optoelectronic Materials and Technology, South China Normal University, Guangzhou 510631, People's Republic of China

Introduction

Lithium (Li) ion batteries containing graphite anodes are now the most widely used power sources for portable electronic devices and electric vehicles [1–3]. However, Li ion batteries with high-specific energy density are in increasing demand in the future commercial applications. Recently, various anode materials have been proposed to deal with the low capacity of graphite (372 mAh g^{-1}) [4–9]. Some attention has been paid to Zn ferrite ($ZnFe_2O_4$) [10–19], a definitely promising candidate as the anode material for Li ion batteries, as for its high theoretical specific capacity (1,072 mAh g^{-1}). However, Pure Zn ferrite as an anode material suffers much from its poor electrical conductivity, cycle ability during Li ion insertion, and extraction [13, 16, 18]. The most prominent problem of Zn ferrite as an anode is the low coulombic efficiency in the first cycle. Therefore, considerable efforts could be made to improve the electrochemical performance of Zn ferrite as an anode material in Li ion batteries [11–21]. On one hand, metallic doping and carbon coating have been proposed as effective ways to enhance their cycle ability. Qin reported the synthesis of Ag-doped $ZnFe_2O_4$ thin films as an anode by a pulsed laser deposition method. The initial reversible capacity was 556 mAh g^{-1} and 78 % of the capacity (434 mAh g^{-1}) was retained over 100 cycles [11]. Deng found that the $ZnFe_2O_4$/C hollow spheres exhibited an initial discharge specific capacity of 1,254 mAh g^{-1} and a reversible specific capacity of 841 mAh g^{-1} could be obtained after 30 cycles at a constant current density of 65 mA g^{-1} [17]. On the other hand, previous researches have proved that the controllable sizes [14, 18] and structure modification [13, 15, 17, 19] could partly alleviate the mechanical stresses induced by the severe volumetric change, which have strong correlation to the electrochemical performance of the anode material.

Chowdari synthesis $ZnFe_2O_4$ using a urea combustion method. The total first-charge capacity is 810 mAh g^{-1} and it could maintain at 615 mAh g^{-1} at a current of 60 mAg^{-1} after 50 cycles [14]. Yang found that the capacity of nanostructured $ZnFe_2O_4$ via the simple polymer pyrolysis method could maintain at over 800 mAh g^{-1} after 50 cycles (with a current of 116 mA g^{-1}) [15]. Recently, Ju reported the hydrothermal synthesis of $ZnFe_2O_4$ octahedrons using toxic material of $N_2H_4{\cdot}H_2O$, getting a high capacity of 910 mAh g^{-1} at 60 mA g^{-1} after 80 cycles [19].

Generally speaking, preparation methods mentioned above have both advantages and disadvantages. Some of them involve sophisticated equipment, high temperature, complicated procedures, rigorous experimental conditions, or toxic substances. Some methods get low yields. It is well known that hollow spherical structure is preferable as a means of improving the anode characteristics due to its high tapping density and buffer effects [22, 23]. Herein, a facile bubble assisted synthesis method is reported to fabricate porous hollow Zn ferrite microspheres as an anode material in Li ion batteries. On one side, the suitable morphology modification can accommodate to volume expansion, supply more reaction sites on the surface and shorten diffusion length for Li-ions as well as electrons. Consequently, it is beneficial to improving electrochemical performance of Zn ferrite as an anode material in Li ion battery. On the other side, the primary materials in our experiments are very cheap and widely available. Most importantly, the electrochemical performance is good and all the materials used are environmentally friendly. The yield is relatively higher and the reaction conditions are suitable for commercial production.

Experimental

Preparation and characterization of porous hollow spherical $ZnFe_2O_4$ electrode

All chemicals used in the experiment were of analytical grade and didn't get any purification. Uniform monodispersed sphere $ZnFe_2O_4$ with porous hollow structure were synthesized by hydrothermal reaction using hydrated iron chloride ($FeCl_3{\cdot}6H_2O$) and zinc chloride ($ZnCl_2$), as raw material, the mixture of ethylene glycol (EG) and deionic water (DI) as solvent solution and dispersing agent, ammonium acetate (NH_4Ac) as protective agent. Firstly, 16 mmol $ZnCl_2$, 32 mmol $FeCl_3{\cdot}6H_2O$, and 60 mmol NH_4Ac were dissolved in a mixture of EG and DI (V_{EG}/V_{DI}=9:1, the total volume was 100 ml) with constant stirring for 1 h. Subsequently,the mixed solution was transferred into a Teflon-lined stainless steel autoclave with a capacity about 150 mL and maintained at 200 °C for 36 h to get the precipitate of $ZnFe_2O_4$. Finally, the obtained $ZnFe_2O_4$ was calcined at 500 °C for 4 h in air. The crystal structure and morphology of the as-prepared products were characterized by X-ray diffraction (XRD; PANalytical X'Pert PRO, Cu $K\alpha$ radiation,λ=1.5406 nm), scanning electron microscopy (SEM; ZEISS ULTRA 55) and transmission electron microscopy (TEM; JEM-2100HR).

Electrochemical performance

The electrochemical performance was tested by using coin-type half-cells (CR2530) assembled in an argon-filled glove box. Working electrodes, with a composition of 75 wt.% $ZnFe_2O_4$, 10 wt.% acetylene black, and 15 wt.% LA132 on the copper foil of 10 μm thickness, were dried at 80 °C for 12 h under vacuum and subsequently pressed. The electrolyte was 1.0 M $LiPF_6$ in a mixture of ethylene carbonate, diethyl carbonate, and ethyl methyl carbonate (1:1:1 by volume, provided by Chei Industries Inc., South Korea). The separator was made of a Celgard 2400 film.

The cycling performance of the cell was evaluated in a constant current mode at a current density of 100 mAh g^{-1} in the voltage range of 0.001–2.5 V (versus Li/Li^+). In this report, the lithiation was expressed as discharging, whereas the de-lithiation as charging. Cyclic voltammetry measurements were performed using electrochemical workstation (Shanghai Chenhua Instrument Co.) at a scan rate of 0.1 mV/s in the range of 0.0–2.5 V.

Results and discussion

The XRD pattern of $ZnFe_2O_4$ powders annealed at 500 °C (Fig. 1) reveals the formation of compound in phase pure form with the cubic spinel structure, and all peaks position received from XRD are conformed with the standard values of the crystalline $ZnFe_2O_4$ (JCPDS Card #01-1109). From the spectrum, it is obvious that no crystalline impurities related to the reaction by-products or to the excess of NH_4Ac are detected. Furthermore, no peaks corresponding

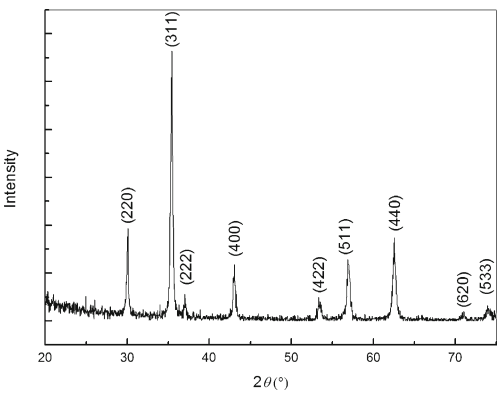

Fig. 1 XRD spectra of porous hollow Zn ferrite spheres annealed at 500 °C

with ZnO and Fe_2O_3 are observed, demonstrating the yields of high purity crystalline of Zn ferrites. The lattice parameter, evaluated by least squares fitting using the 2θ and *hkl* values, is a=8.427 Å and is in good agreement with the reported value of 8.441 Å.

The morphologies of the prepared $ZnFe_2O_4$ samples are characterized by SEM and TEM, and the images are illustrated in Fig. 2. It is obvious here that $ZnFe_2O_4$ particles share some uniform distribution in size on matter it is annealed or not. Egg-like spheres with an average diameter of 300–400 nm are observed (Fig. 2a). The broken microspheres of Zn ferrite as an anode illustrated in Fig. 2b, indicate that the products consist of spherical hollow particles. Further information is shown in Fig. 2c, d. The hollow inside the Zn ferrite sphere (Fig. 2c) can be clearly observed. With a careful inspection (Fig. 2c, d), it is noted that hollow spheres have relatively rough surface and are composed of small primary $ZnFe_2O_4$ grains. Moreover, there are some openings and holes produced by the aggregation of Zn ferrite particles on the uneven surface of hollow spheres, which create numerous nanoscale channels for ionic and electronic transport between the interior cavity and exterior space, thus making the hollow spheres particularly suitable for the Li^+ insertion and extraction. Especially, due to the relatively stable loose structure, porous hollow sphere can serve as a buffer and sufficiently alleviate the mechanical stress caused by the large volume change, which causes cracking and crumbling of the electrode material and result in great capacity loss during the charge–discharge process. The big difference between Fig. 2c, d is that the annealed $ZnFe_2O_4$ shows higher crystallinity. The structure of annealed particles is more stable. In our experimental process, we found that the size of $ZnFe_2O_4$ was partially depended on the density of solvent solution. When the EG and DI was used as solvent with a volume ratio of 1:1, the diameter of $ZnFe_2O_4$ particles reduced significantly (Fig. 2e). It comes to form the solid $ZnFe_2O_4$ nanoparticles of a few tens of nanometers instead of hollow structure. Additionally, the concentration of NH_4Ac, temperature, and the hydrothermal reaction time is connected to the morphology and size of the final $ZnFe_2O_4$ products [24–26]. With a similar synthesis condition, Yuan have confirmed the existence of NH_3 bubbles using the method of gas chromatography during the hydrothermal reaction [26] (Fig. 3).

Based on the above-experimental results and previous reports, the possible bubble-assisted formation mechanism is proposed (Fig. 4). With the temperature increasing, the

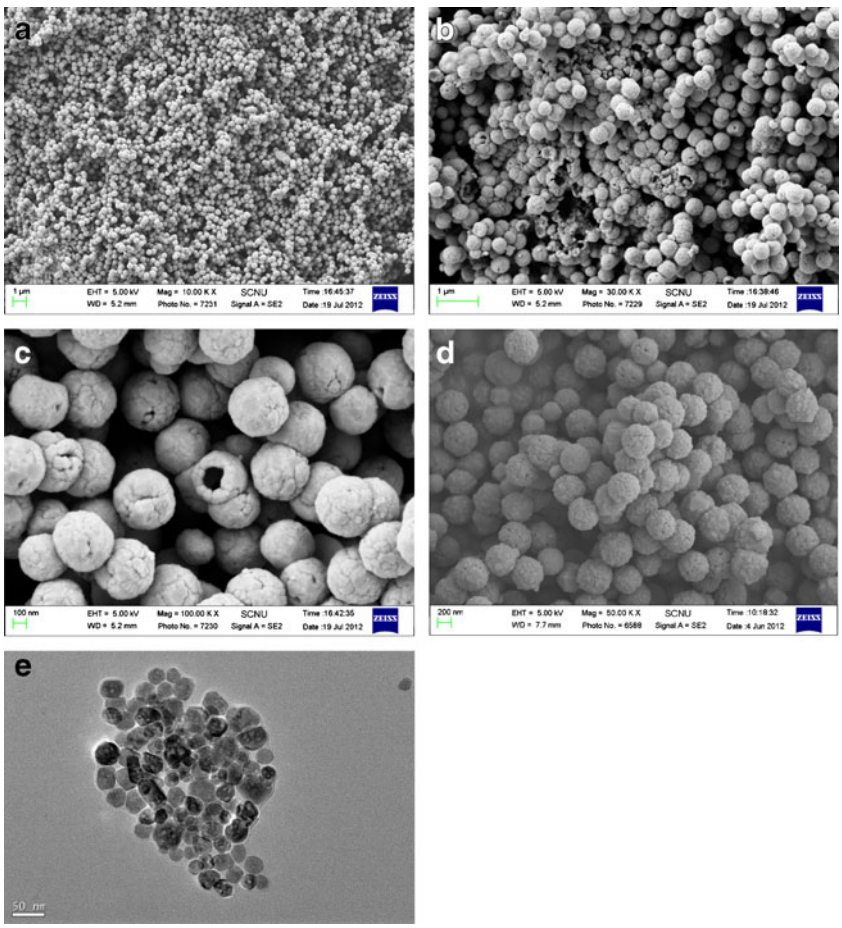

Fig. 2 Representative SEM images of the porous hollow $ZnFe_2O_4$ particles as synthesized at 200 °C for 36 h by hydrothermal method (**a**–**c**) and then annealed at 500 °C (**d**); TEM images of $ZnFe_2O_4$ particles by using different volume ratio of V_{EG}/V_{DI} (1:1)

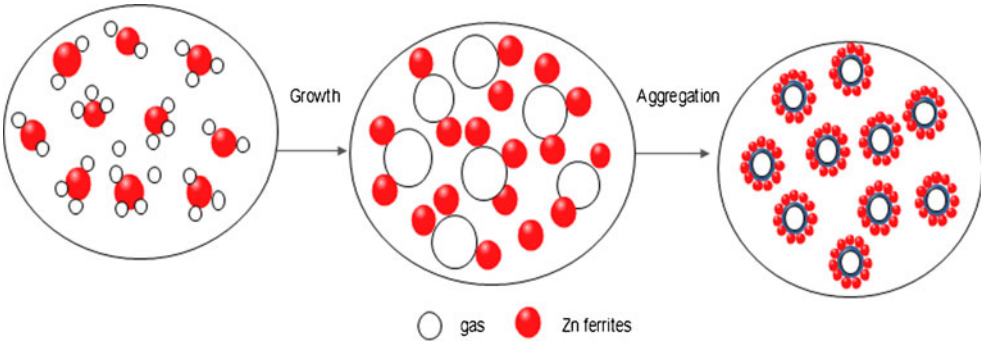

Fig. 3 Synthesis process of porous hollow Zn ferrite spheres

primary bubbles are produced by the thermal decomposition of NH_4Ac [27], simultaneously the small gas bubbles were generated in the dispersion system (the mixture of EG and DI) to form bigger bubbles (several hundreds of nanometer), getting a low thermodynamic free energy, and then providing an assembly spherical template for the deposition of Zn ferrite precursors during the reaction. Meanwhile, a nucleation process takes place at the liquid–gas interface. Bubbles acted as aggregation center and the fresh-formed unstable crystalline Zn ferrite nucleus are absorbed thermodynamically on the gas/solution interface driven by the minimization of interfacial free energy and form hollow structure finally [28–30]. With the continuous aggregation process, more and more Zn ferrite precursors aggregate, leading to the thickness of shells and hollow structure. When the force of gravity is greater than the total buoyancy and the interfacial force acting on the particle in liquid, the sphere would sink to the button of Teflon-lined stainless steel autoclave. However, if the density of solution is too low, the small $ZnFe_2O_4$ particles will sink to the button directly other than aggregating on the surface of bubbles. It should be mentioned here that it was an unexpected finding of pores on the uneven surface of spheres. What causes the porous structure might be related to the instability and fluidity of the gas in the whole process of reaction.

Figure 4 shows the charge–discharge voltage profiles and cycling performance of porous hollow $ZnFe_2O_4$ spheres as anode material in Li ion battery. The high initial discharge and charge specific capacity of the $ZnFe_2O_4$ spheres are approximately 1,400 and 1,000 mAh g^{-1}, respectively. The electrode has a large irreversible capacity at the first charge–discharge process and the coulombic efficiency at the first cycle is 71 %. Two conceivable mechanisms are suggested: Li-ions are trapped in the interstitials of Li_2O irreversibly, or small amounts of impurity phases are reacted irreversibly. In addition, this irreversibly capacity can be ascribed mainly to the formation of solid electrolyte interface (SEI) film. The formation of the film is closely related to the surface area. Many Li ions would be consumed irreversibly to form the SEI film as for the hollow structure has large specific surface area. As a result, the initial irreversible capacity is relatively high. To understand the irreversible mechanism, detailed structural investigation and lithium/de-lithium theoretical mechanism are required. We intend to investigate this point in the near future. To our surprise, a reversible capacity of 584 mAh g^{-1} can be maintained after 100 cycles at a constant current density of 100 mA g^{-1}.

In the initial discharge curves, it can be divided into three regions: regions A (2.5–0.8 V), B (0.8–0.6 V), and C (0.6–

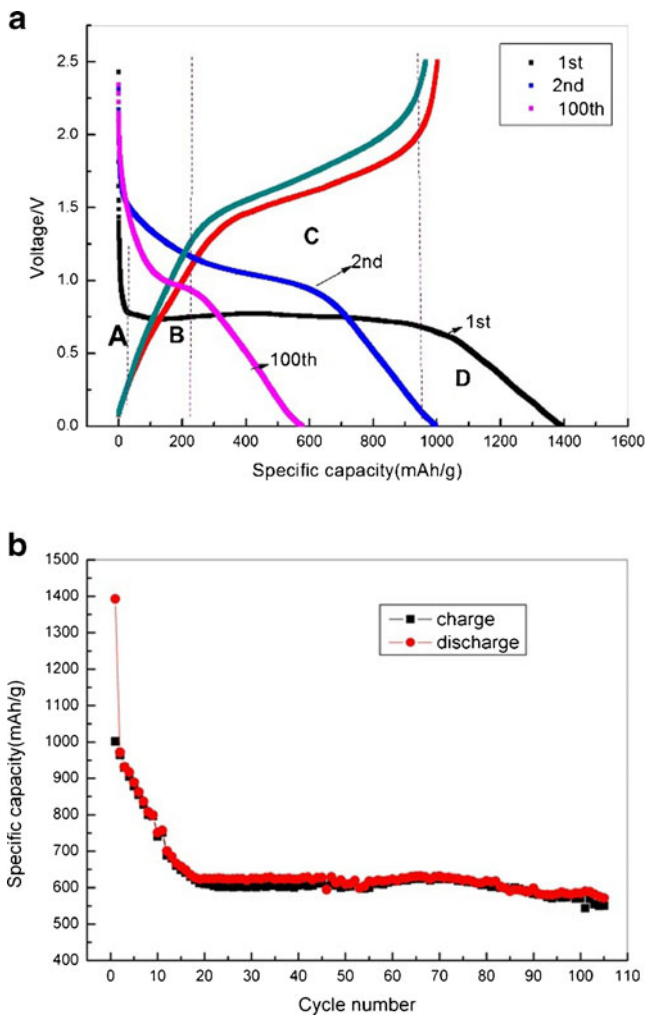

Fig. 4 **a** Charge–discharge performance of Zn ferrite electrode at a constant current density of 100 mAh g^{-1} and **b** cycling performance of porous hollow Zn ferrite spheres annealed at 500 °C

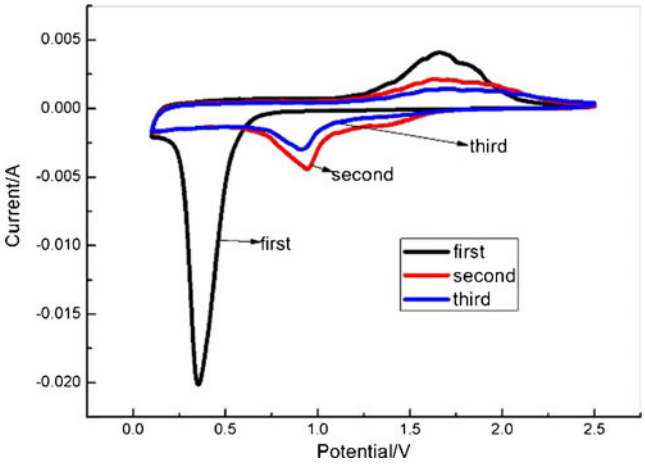

Fig. 5 The cyclic voltammetry plots of the Zn ferrite in the potential range of 0.0–2.5 V at the scan rate of 0.1 mV/s

0.01 V). There exhibits two obvious voltage plateaus including a short one at 0.7 V and a long one at 0.75 V, and is unconspicuous in the following discharge profiles, which seems to have been changed into two slopes at 2.5–1.0 and 1.0–0.01 V. In the A area, the voltage presents a drastic drop, subsequently, shows up a distinct inflection point at 0.8 V, and a short voltage plateau in area B is evident, which can be attributed to the formation of $Li_{0.5}ZnFe_2O_4$ [13]. The following long-voltage plateau is corresponded to the composition of $Li_2ZnFe_2O_4$,which extends up to a consumption of 6.0 mol Li^+ along with incomplete reduction of Fe^{3+}, Fe^{2+}, and Zn^{2+} to Fe^0 and Zn^0 as well as the formation of amorphous Li_2O. As the voltage declines gradually up to the 0.01 V, a whole initial discharge specific capacity of 1,400 mAh g^{-1} is noted, which may be associated with the further reduction, the formation of Li–Zn alloy and the irreversible decomposition of the solvent in the electrolyte to form SEI on the electrode surface. As can be seen from the plot of cycle performance (Fig. 4b), the specific capacity is not stable and decays gradually in the previous 20 cycles. When the Li diffusion and electrochemical kinetics reach an optimal state, it stabilized at a high lever with specific capacity of more than 600 mAh g^{-1} and then after 100 cycles it also maintained as high as 584 mAh g^{-1}. The reasons may be as follows:

Firstly, the uniform porous hollow spherical structure with mean size 300–400 nm offers improves kinetic properties, which shorter diffusion length for ionic and electronic transport. Secondly, the spheres provide large electrode/electrolyte contact area for ions and electrons. Lastly, the hollow structure could serve as a buffer to restrain the volume changes during the Li insertion and de-insertion. As a result, the porous hollow Zn ferrite exhibits a good cyclic retention and improved reversible capacity. Some researchers have reported the Li storage mechanism of $ZnFe_2O_4$ [13]. The discharge and charge process reaction are as follows:

$$ZnFe_2O_4 + 0.5Li^+ + 0.5e^- \rightleftarrows Li_{0.5}ZnFe_2O_4$$
$$Li_{0.5}ZnFe_2O_4 + 1.5Li^+ + 1.5e^- \rightleftarrows Li_2ZnFe_2O_4$$
$$Li_2ZnFe_2O_4 + 6Li^+ + 6e^- \rightarrow 4Li_2O + Zn + 2Fe$$
$$Zn + Li^+ + e^- \rightleftarrows LiZn$$
$$3Li_2O + 2Fe \rightleftarrows Fe_2O_3 + 6Li^+ + 6e^-$$
$$Li_2O + Zn \rightleftarrows ZnO + 2Li^+ + 2e^-$$

In order to investigate the electrochemical mechanism of the Li ion insertion and extraction reaction, cyclic voltammograms (CVs) of the sample is shown in Fig. 5. There are multiple peaks and activation processes in the CV curves of Zn hollow ferrite. In the first cycle ,an characteristic cathodic peaks at 0.4 V could be ascribed to the reduction of Fe^{3+}, Fe^{2+}, and Zn^{2+} to Fe^0 and Zn^0,while two anodic peaks at 1.7 and 1.8 V corresponded to the electrochemical Li insertion reactions with the reversible oxidation of $Fe^0$and Zn^0 to Fe^{3+}, Fe^{2+}, and Zn^{2+}. It should be mentioned that the wide peak located at 0.4 V disappeared in the subsequent cycles, indicating the larger initial reversible capacity losing, which could be related to electrolyte decomposition, electrode polarization, and SEI film formation on the surface of porous hollow Zn ferrite spheres. Because of the formation process of SEI film, many Li^+ and charges would be consumed, leading to the appearance of the initial slightly larger capacity loss in the first cycle. Once the SEI film is formed, the cathodic peaks in the following cycles are stabilized approximately at 1.0 V which is well in agreement with the discharge potential plateau in Fig. 5. On the other hand, compared with the first cycle, it is apparently found that in the anodic part of CV, the potential peaks broaden, the current decreases, and the integrated area shrinks, which indexed to the initial irreversible capacity loss . However, the area reduced a little from the second cycle and maintains almost the same, demonstrating the good cycle ability of the porous hollow Zn ferrite as an anode in Li ion batteries.

Conclusions

In summary, a environmentally friendly, economical, and relatively high-yield method was introduced successfully to fabricate a new porous and hollow Zn ferrite sphere as an anode material for Li-ion battery, and a possible bubble-assisted formation mechanism was proposed to explain the fabrication of the porous hollow spherical structure. As an anode material for Li ion battery, the porous hollow Zn ferrite anode exhibited excellent electrochemical performance. The high initial discharge- and charge-specific capacity of the $ZnFe_2O_4$ anode were approximately 1,400 and 1000 mAh g^{-1}, respectively, showing an initial efficiency of 71 %. Furthermore, a reversible capacity of 584 mAh g^{-1} can be maintained after 100 cycles at a constant current density of 100 mA g^{-1}. The good cyclic

retention of $ZnFe_2O_4$ could be ascribed to the porous hollow nanospherical morphology. First, the specific loose structure serves as a buffer and partially alleviate the sever volume change during the reaction. Second, the holes on the sphere provide large electrode/electrolyte contact area and shorten diffusion length for ions and electrons, consequently improving the kinetics of the electrochemical reaction. The high capacity and stable cycling performance of porous Zn ferrite hollow microspheres indicate that the suitable internal structure could be an effective way to improve the electrochemical properties of anode materials in Li ion batteries. With the economical, simple, environmentally friendly synthetic strategy, and excellent electrochemical behavior, it is believed that the Zn ferrite have the great potential to be considered as an alternative anode material for Li-ion batteries.

Acknowledgment This work was financially supported by the Scientific Research Foundation of Graduate School of South China Normal University, the National Science Foundation of China (NSFC; No. 51201066, 51171065, and11204090), China Postdoctoral Science Foundation funded project (2012T50733), Guangdong Natural Science Foundation (No. S2012020010937), and the Scientific and Technological Plan of Guangdong Province (No. 2011B010400022 and 2011J4100075).

References

1. Scrosati B (2000) Electrochim Acta 45:2461–2466
2. Wakihara M (2001) Mater Sci Eng R33:109–134
3. Casas CL, Li WZ (2012) J Power Sources 208:74–85
4. Li XL, Yoon SH, Dua K, Zhang YX, Huang JM, Kang FY (2010) Electrochim Acta 55:5519–5522
5. Gu P, Cai R, Zhou Y, Shao ZP (2010) Electrochim Acta 55:3876–3883
6. Huang L, Cai JS, He Y, Ke FS, Sun SG (2009) Electrochem Commun 11:950–953
7. Cui WJ, Wang F, Wang J, Liu HJ, Wang C, Xia YY (2011) J Power Sources 196:3633–3639
8. Sarakonsri T, Johnson CS, Hackney SA, Thackeray MM (2006) J Power Sources 153:319–327
9. Li H, Wang Q, Shi LH, Chen LQ, Huang XJ (2002) Chem Mater 14:103–108
10. Cherian CT, Reddy MV, Subba Rao GV, Sow CH, Chowdari BVR (2012) J Solid State Electrochem 16:1823–1833
11. NuLi Y, Chu YQ, Qin QZ (2004) J Electrochem Soc 151:A1077–A1083
12. Zahi S, Daud AR, Hashim M (2007) Mater Chem Phys 106:452–456
13. Guo XW, Lum X, Fang XP, Mao Y, Wang ZX, Chen LQ, Xu XX, Yang H, Liu YN (2010) Electrochem Commun 12:847–850
14. Bahout MM, Bertrand S, Pena O (2005) J Solid State Chem 178:1080–1086
15. Ding Y, Yang YF, Shao HX (2011) Electrochim Acta 56:9433–9438
16. Sharma Y, Sharma N, Subba Rao GV, Chowdari BVR (2008) Electrochim Acta 53:2380–2385
17. Deng YF, Zhang Q, Tang SD, Zhang LT, Deng SN, Shi ZC, Chen GH (2011) Chem Commun 47:6828–6830
18. Xu HY, Xl C, Chen L, Li LE, Xu LQ, Yang J, Qian YT (2012) Int J Electrochem Sci 7:7976–7983
19. Xing Z, Ju ZC, Yang J, Xu HY, Qian YT (2012) Nano Res 5(7):477–485
20. Hassoun J, Lee KS, Sun YK, Scrosati B (2011) J Am Chem Soc 133:3139–3143
21. Ortiz G, Tirado JL (2011) Electrochem Commun 13:1427–1430
22. Jiang DH, Hu WB, Wang HR, Shen B, Deng YD (2012) Chem Eng J 189:443–450
23. Luo M, Liu Y, Hu JC, Li JL, Liu J, Richards RM (2012) Appl Catal Environ 125:180–188
24. Wang HZ, Liang JB, Fan H, Xi BJ, Zhang MF, Xiong SL, Zhu YC, Qian YT (2008) J Solid State Chem 181:122–129
25. Yan AG, Liu XH, Yi R, Shi RR, Zhang N, Qiu GZ (2008) J Phys Chem C112:8558–8563
26. Hu P, Yu LJ, Zuo AH, Guo CY, Yuan FL (2009) J Phys Chem C 113:900–906
27. Oommen C, Jain SR, Hazard J (1999) Mater A67:253–281
28. Israelachvili J, Wennerström H (1996) Nature 379:219–225
29. Matijevic E (1993) Chem Mater 5:412–426
30. Matijevic E (1994) Langmuir 10:8–16